Role of Guanine Nucleotides in the Vinblastine-Induced Self–Association of Tubulin: Effects of Guanosine α,β–Methylenetriphosphate and Guanosine α,β–Methylenediphosphate †

3 AUTHORS, INCLUDING:

Sharon Lobert
University of Mississippi Medical Center
49 PUBLICATIONS **959** CITATIONS

SEE PROFILE

John Correia
University of Mississippi Medical Center
114 PUBLICATIONS **3,552** CITATIONS

SEE PROFILE

Role of Guanine Nucleotides in the Vinblastine-Induced Self-Association of Tubulin: Effects of Guanosine α,β-Methylenetriphosphate and Guanosine α,β-Methylenediphosphate[†]

Bojana Vulevic,[‡] Sharon Lobert,[§] and John J. Correia*,[‡]

Department of Biochemistry and School of Nursing, University of Mississippi Medical Center, Jackson, Mississippi 39216

ABSTRACT: It is now well established that guanine nucleotides are allosteric effectors of the vinca alkaloid-induced self-association of tubulin. GDP enhances self-association for vinblastine-, vincristine- and vinorelbine-induced spiral assembly relative to GTP by 0.90 ± 0.17 kcal/mol [Lobert et al. (1996) *Biochemistry 35*, 6806−6814]. Since chemical modifications of the vinca alkaloid structure are known to modulate the overall affinity of drug binding, it is very likely that, by Wyman linkage, chemical modifications of guanine nucleotide allosteric effectors also modulate drug binding. Here we compare the effects of the GTP and GDP α,β-methylene analogues GMPCPP and GMPCP on vinblastine-induced tubulin association in 10 and 100 mM piperazine-*N*,*N*′-bis(2-ethanesulfonic acid) (Pipes), 1 mM MgSO$_4$, and 2 mM [ethylenebis(oxyethylenenitrilo)]tetraacetic acid (EGTA), pH 6.9, at different temperatures. We found that GMPCPP perfectly mimics GTP in its effect on spiral assembly under all ionic strength and temperature conditions. However, GMPCP in 10 mM Pipes behaves not as a GDP analogue, but as a GTP analogue. In 100 mM Pipes, GMPCP has characteristics that are intermediate between GDP and GTP. These data suggest that the α,β methylene group in GMPCP and GMPCPP is sufficient to produce a GTP-like effect on vinblastine-induced tubulin self-assembly. This is consistent with previous observations that GMPCP-tubulin will assemble into microtubules in a 2 M glycerol and 100 mM Pipes buffer [Vulevic & Correia (1997) *Biophys. J. 72*, 1357−1375]. Our results demonstrate that an α,β methylene modification of the guanine nucleotide phosphate moiety can induce a salt-dependent conformational change in the tubulin heterodimer that favors the GTP-tubulin structure. This has important implications for understanding allosteric interactions that occur in the binding of guanine nucleotides to tubulin.

The antimitotic drug vinblastine inhibits microtubule assembly and induces the self-association of tubulin into coiled spiral aggregates. Vinblastine-induced self-association of tubulin is best described by a mechanism involving isodesmic ligand-mediated or ligand-mediated plus ligand-facilitated self-assembly (*1*). In the presence of GDP, vinca alkaloid induced-spiral assembly is enhanced compared to assembly in the presence of GTP (*1*, *2*). The enhancement is manifested in K_2, the affinity of liganded heterodimers for spiral polymers, and in K_3, the binding of the drug to unliganded polymers. Overall enhancement, K_1K_2, for vinblastine, vincristine, and vinorelbine is 0.90 ± 0.17 kcal/mol and corresponds to a 3−5-fold increase in GDP- over GTP-tubulin association. Thus, guanine nucleotides are allosteric effectors in the interaction of vinca alkaloids with tubulin. These observations are consistent with the hypothesis that vinca alkaloids depolymerize microtubules by first binding to the ends of microtubules, the so-called GTP-tubulin cap, and then by inducing enhanced spiral propagation into the GDP core of the microtubule (*2*−*4*). Vinca alkaloid-induced spiral assembly is known to be dependent upon solution conditions such as buffer composition, ionic strength, and Mg^{2+} concentrations (*3*, *5*−*8*). The addition of 50−150 mM NaCl enhances vinblastine−tubulin self-association (*8*). Enhancement is larger in the presence of GTP versus GDP, consistent with electrostatic inhibition in the GTP-tubulin state. Surprisingly, salt suppresses the induction of larger amorphous aggregates and reduces the formation of paracrystals and the precipitation of tubulin induced by other divalent cations like Mn^{2+} and Ca^{2+}. This is most probably achieved by screening of favorable electrostatic interactions that are involved in the lateral association of vinca-induced spirals.

The slowly hydrolyzable GTP analogue GMPCPP[1] has been found to be an effective probe of the role of GTP hydrolysis in microtubule assembly (*9*−*12*). Microtubules assembled in the presence of GMPCPP exhibit variation in lateral bonding between GTP-like subunits (*13*) and changes in the packing density along protofilaments (*14*) relative to microtubules assembled in the presence of GTP. The

---

* To whom correspondence should be addressed: Department of Biochemistry, University of Mississippi Medical Center, 2500 North State St., Jackson, MS 39216. Phone 601-984-1522.

[‡] Department of Biochemistry.

[§] School of Nursing.

[1] Abbreviations: ASA, water-accessible surface area; EGTA, [ethylenebis(oxyethylenenitrilo)]tetraacetic acid; E-site, exchangeable nucleotide binding site located on the β-subunit; GMPCPP and GMPCP, guanosine triphosphate and diphosphate nucleotide analogues where the αβ oxygen has been replaced by a methylene, -CH$_2$-; GXP, guanine nucleotide of the appropriate form; MAPs, microtubule-associated proteins; PC-tubulin, tubulin purified by phosophocellulose chromatography; Pipes, piperazine-*N*,*N*′-bis(2-ethanesulfonic acid); MT, microtubules.

diphosphate form of this analogue, GMPCP, also promotes the formation of microtubules, suggesting that it is not a true GDP analogue (*12*). Van't Hoff analysis of microtubule polymerization induced by GMPCPP and GMPCP suggests a 3−6× larger burial of nonpolar water-accessible surface area (ASA) than in the presence of GTP or taxol (*12*). Entropy analysis indicates this corresponds to additional conformational rearrangement during assembly of GMPCPP- or GMPCP-tubulin. Since vinblastine-induced tubulin self-association is sensitive to modifications in the phosphate moiety of guanine nucleotides (*1, 2, 8*), it seems appropriate to probe this polymerization process with guanine nucleotides modified in the phosphate region. This study investigates the influence of an α,β-methylene on longitudinal spiral formation and asks the question: by the criteria of vinca alkaloid−tubulin interactions, are GMPCPP and GMPCP true GTP and GDP analogues?

In the work described here, we study the interaction of vinblastine with PC-tubulin in the presence of GMPCPP and GMPCP and compare the results with data collected in the presence of GTP and GDP. Experiments were performed at various temperatures in 10 mM Pipes and 100 mM Pipes buffers to explore microtubule nonassembly and assembly promoting conditions. By the criteria of vinblastine-induced tubulin self-association, GMPCPP is a nearly perfect analogue of GTP under all studied conditions. Furthermore, the diphosphate analogue, GMPCP, also acts as a GTP analogue in 10 mM Pipes and a partial GTP analogue in 100 mM Pipes. This is consistent with the previous observation that, unlike GDP, GMPCP will promote microtubule assembly (*12*). An increase in buffer concentration stimulates spiral assembly more in the presence of GTP and GMPCPP than in the presence of GDP, consistent with the conclusion there is a significant inhibitory electrostatic component to the GDP enhancement (*8*). The largest increase in spiral assembly upon an increase in buffer concentration is observed with GMPCP-tubulin, suggesting that the α,β-methylene alone, separate from the γ-phosphate, induces a salt-dependent conformational change in the tubulin heterodimer. This has important implications for the structure of the GXP-tubulin complex and the allosteric interactions mediated by different GXP moieties.

MATERIALS AND METHODS

Reagents. Deionized (Nanopure) water was used in all experiments. MgSO$_4$, EGTA, GDP (Type I), GTP (Type II-S), ADP, Pipes, and vinblastine sulfate were purchased from Sigma Chemical Co. Sephadex G-50 was from Pharmacia. GMPCPP and GMPCP were synthesized in our laboratory (*12*).

Tubulin Purification. Porcine brain tubulin (PC-tubulin) free of MAPs was obtained by two cycles of warm−cold polymerization−depolymerization followed by phosphocellulose chromatography to separate tubulin from MAPs (*15, 16*). Protein concentrations were determined spectrophotometrically, $\epsilon_{278} = 1.2$ L/(g cm) (*17*).

Sedimentation Velocity Experiments. Sedimentation studies were done in a Beckman Optima XLA analytical ultracentrifuge equipped with absorbance optics and an An60 Ti rotor. Self-association of 2 μM PC-tubulin in the presence of vinblastine and GTP, GDP, GMPCPP, GMPCP, ADP, or no nucleotide was studied by sedimentation velocity. For

experiments in GDP, GMPCPP, GMPCP, ADP, or no nucleotide, tubulin samples were rapidly equilibrated (using spun Sephadex G-50 columns), first into 10 or 100 mM Pipes, pH 6.9, and 2 mM EGTA to remove GTP bound at the exchangeable site (*1, 16*). A second equilibration was done in 10 or 100 mM Pipes, pH 6.9, 2 mM EGTA, 1 mM MgSO$_4$, and 50 μM GDP, GMPCP, GMPCPP, ADP, or no nucleotide and vinblastine concentrations ranging from 0.05 to 75 μM. Because GMPCP binds to tubulin with low affinity (*11*), in a number of experiments (indicated as GMPCP* in the text and Table 1) tubulin was first equilibrated into 10 or 100 mM Pipes, pH 6.9, 2 mM EGTA, and 1 mM GMPCP and then into 10 or 100 mM Pipes, pH 6.9, 1 mM MgSO$_4$, 2 mM EGTA, and 1 mM GMPCP prior to equilibration into 50 μM GMPCP, 1 mM MgSO$_4$, 2 mM EGTA, 10 or 100 mM Pipes, pH 6.9, and appropriate vinblastine concentrations. This was to ensure complete exchange of GMPCP for bound GTP/GDP. [Note that measurement of GMPCP binding by HPLC (*16, 18*) is not directly possible because weak binding nucleotides do not stay bound during the separation method (J. J. Correia, unpublished observations).] For experiments with GTP-tubulin, samples were equilibrated only in 10 or100 mM Pipes, pH 6.9, 2 mM EGTA, 1 mM MgSO$_4$, 50 μM GTP buffer, and appropriate drug concentrations as above. The free drug concentration (0.05−75 μM) was obtained from the known drug concentration in the equilibration buffer. After equilibration, the protein was brought to the desired final concentration by dilution with an appropriate equilibration buffer. In 100 mM Pipes, samples were spun in a Beckman XLA analytical ultracentrifuge at 5 and 19.7 °C since tubulin assembles into microtubules in the presence of GMPCPP at temperatures > 20 °C (*12*). Note that, even at these temperatures, caution must be exercised when working with GMPCPP to not obtain too high a tubulin concentration, or otherwise microtubules will form during sample preparation. In 10 mM Pipes, samples were spun at 5 and 24.7 °C. [Above 30 °C tubulin readily formed small aggregates even in the absence of vinca alkaloids. The presence of these larger species interfere with quantitative analysis. These species may represent microtubule nuclei or denatured tubulin, depending upon the solution conditions. A thorough analysis of these tubulin aggregates above 30 °C will be presented elsewhere (Vulevic, Lobert, and Correia, manuscript in preparation).] Ultracentrifugal speeds were between 16 000 and 42 000 rpm. Temperature was calibrated by method of Liu and Stafford (*19*). Velocity data were collected at 278 nm and at a spacing of 0.002 cm with one average in a continuous scan mode. Data were analyzed using the software (DCDT) provided by Dr. Walter Stafford (Boston Biomedical Research Institute) to generate a distribution of sedimentation coefficient, $g(s)$, as described previously (*1, 20*).

Curve Fitting of Sedimentation Velocity Data. The sedimentation data were plotted as weight average $\bar{s}_{20,w}$ vs free drug concentration. Total protein concentration in the plateau was determined from $\int g(s) \, ds$. Sedimentation data were fit using the isodesmic ligand-mediated or isodesmic ligand-mediated plus -facilitated model (also referred to as a combined model) as previously described (*1*). In these models, K_1 is the affinity of drug X for tubulin heterodimers A, K_2 is the affinity of liganded heterodimers AX for polymers, K_3 is the affinity of ligand for polymers, and K_4
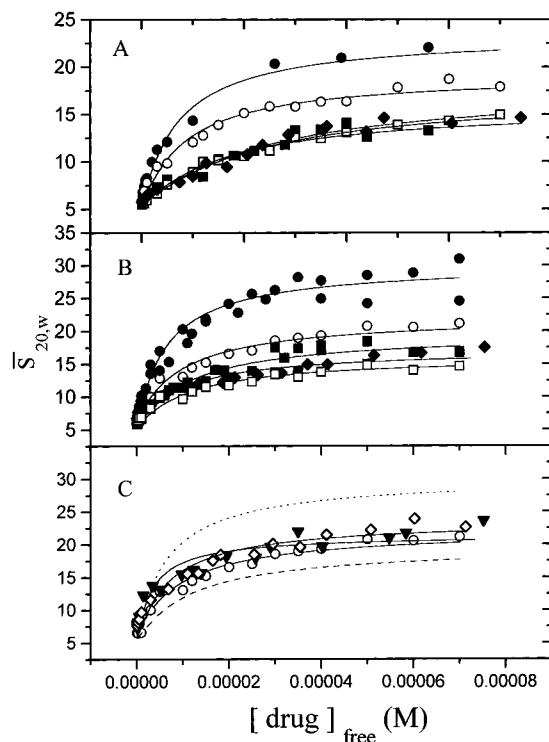
FIGURE 1: Plots of $\bar{s}_{20,w}$ values vs free vinblastine concentrations. Initial tubulin in all experiments was 2 μM. GMPCP* stands for additional equilibration of tubulin in 1 mM GMPCP containing buffers, as described in Materials and Methods. The buffers were 10 mM Pipes, pH 6.9, 1 mM MgSO$_4$, 2 mM EGTA, and 50 μM GXP. The lines represent fits using the combined ligand-mediated plus -facilitated model with K_4 constrained to be 1 × 10^4 M^{-1}. Panel A: Experiments at 5 °C in the presence of GDP (●), GMPCP (○), GTP (■), GMPCPP (□), or GMPCP* (◆). Panel B: Experiments at 24.7 °C in the presence of GDP (●), GMPCP (○), GTP (■), GMPCPP (□) or GMPCP* (◆). Panel C: Experiments at 24.7 °C in the presence of ADP (◇) or no nucleotide (▼). The data with GMPCP (○) and the fits of the GDP(···) and the GTP (- - -) data from panel B are plotted for relative comparison.

FIGURE 2: Plots of $\bar{s}_{20,w}$ values vs free vinblastine concentrations. Initial tubulin in all experiments was 2 μM. GMPCP* stands for additional equilibration of tubulin in 1 mM GMPCP containing buffers, as described in Materials and Methods. The buffers were 100 mM Pipes, pH 6.9, 1 mM MgSO$_4$, 2 mM EGTA, and 50 μM GXP. The lines represent fits using the combined ligand-mediated plus -facilitated model with K_4 constrained to be 1 × 10^4 M^{-1}. Panel A: Experiments at 5 °C in the presence of GDP (●), GMPCP (○), GTP (■), GMPCPP (□), or GMPCP* (◆). Panel B: Experiments at 19.7 °C in the presence of GDP (●), GMPCP (○), GTP (■), GMPCPP (□) or GMPCP* (◆).

RESULTS

The association of 2 μM PC-tubulin in the presence of vinblastine, ranging from 0.05 to 75 μM, and 50 μM GXP (GMPCPP, GMPCP, GTP, and GDP) was studied by sedimentation velocity. The data were collected in 10 and 100 mM Pipes. $\bar{s}_{20,w}$ values were calculated and plotted against free drug concentration at 5 and 24.7 °C in low buffer concentration (Figure 1) and at 5 and 19.7 °C in high buffer concentration (Figure 2). Binding parameters were obtained by fitting data with ligand-mediated and combined ligand-mediated plus -facilitated models (Table 1). Solid lines in Figure 1 and 2 represent combined fits of the data. As reported previously, vinblastine-induced spiral assembly is enhanced in the presence of GDP compared to GTP. The overall GDP enhancement [$\Delta\Delta G(K_1 K_2)$], averaged over both temperatures, corresponds to 0.96 (±0.20) kcal/mol in 10 mM Pipes, while in 100 mM Pipes it decreases to 0.43 (±0.17) kcal/mol. A similar reduced enhancement was found upon addition of 150 mM NaCl (8). GDP enhancement under both buffer conditions occurs primarily in K_2, the binding of liganded heterodimers to spirals, and in K_3, the binding of drug to spiral polymers. Since GDP enhancement [$\Delta\Delta G(K_1 K_2)$], is temperature-independent, this implies that the effect of temperature on GDP- and GTP-tubulin is similar while the absolute differences observed under different nucleotide and vinca conditions remain the same.

There is no significant difference in the vinblastine-induced self-association of GMPCPP-tubulin relative to GTP-tubulin. This is evident by the superposition of $\bar{s}_{20,w}$ data (■, □) under

is the association constant for unliganded tubulin heterodimers, as shown in the scheme below. In Figures 1−4, the lines represent fits using the combined ligand-mediated plus facilitated model with K_4 constrained to be 1 × 10^4 M^{-1}. Binding constants were obtained by fitting with the nonlinear least-squares program Fitall (MTR Software, Toronto, Canada), modified to include the appropriate fitting functions.

$$2A + 2X \underset{K_1}{\rightleftharpoons} 2AX$$
$$K_4 \Updownarrow \qquad \Updownarrow K_2$$
$$A_2 + 2X \underset{K_3}{\rightleftharpoons} A_2X_2$$
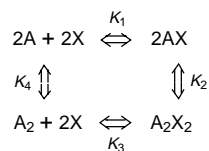
To verify the reliability of these measurements, we have repeated the sedimentation velocity studies of Lobert et al. (1) at 24.7 °C in 10 mM Pipes, 1 mM MgSO$_4$, and 2 mM EGTA, pH 6.9, plus 50 μM GDP and GTP. The new data are presented as a composite plot with the original data from Lobert et al. (1), and both global and individual fits of the data give identical results (Figure 1B and Table 1, global fits labeled with footnote *d*). This verifies that the results are highly reproducible when conducted with fresh buffers on different tubulin preparations by different individuals in the laboratory at different times.
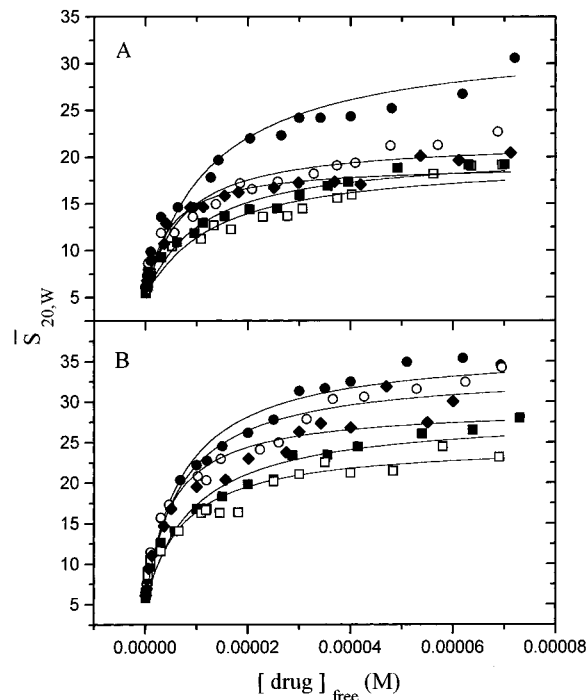
Table 1: Equilibrium Constants for the Interactions of Vinblastine with Tubulin in the Presence of Different Guanine Nucleotides and Buffers Concentrations[a]

GXP	K_1 (M^{-1})	K_2 (M^{-1})	K_3 (M^{-1})	K_1K_2 (M^{-2})	SD
		10 mM Pipes Buffer, 5.0 °C			
GTP[b]	3.4×10^4 (± 1.0)	2.0×10^5 (± 0.04)	6.8×10^5 (± 2.0)	6.8×10^9	0.8
	4.7×10^4 (± 1.0)	4.1×10^6 (± 0.2)		1.9×10^{11}	0.5
GMPCPP	3.8×10^4 (± 0.03)	2.3×10^5 (± 0.03)	8.6×10^5 (± 0.04)	8.6×10^9	0.4
	4.8×10^4 (± 0.5)	4.6×10^6 (± 0.4)		2.2×10^{11}	0.3
GDP[b]	1.2×10^5 (± 0.1)	3.2×10^5 (± 0.08)	4.0×10^6 (± 0.3)	4.0×10^{10}	0.8
	1.5×10^5 (± 0.2)	1.0×10^7 (± 0.1)		1.5×10^{12}	0.9
GMPCP	1.0×10^5 (± 0.01)	2.6×10^5 (± 0.04)	2.6×10^6 (± 0.01)	2.6×10^{10}	0.6
	1.1×10^5 (± 0.1)	6.4×10^6 (± 0.5)		7.0×10^{11}	0.7
GMPCP*[c]	4.4×10^4 (± 1.0)	2.1×10^5 (± 0.04)	9.2×10^5 (± 2.0)	9.2×10^9	0.5
	5.4×10^4 (± 0.1)	4.3×10^6 (± 0.5)		2.3×10^{11}	0.5
		10 mM Pipes Buffer, 24.7 °C			
GTP[d]	7.4×10^4 (± 0.07)	2.6×10^5 (± 0.04)	1.9×10^6 (± 0.01)	1.9×10^{10}	1.0
	9.0×10^4 (± 1.3)	6.1×10^6 (± 0.6)		5.5×10^{11}	1.0
GMPCPP	8.0×10^4 (± 0.3)	1.9×10^5 (± 0.1)	1.6×10^6 (± 0.04)	1.6×10^{10}	0.7
	1.0×10^5 (± 0.2)	3.5×10^6 (± 0.5)		3.6×10^{11}	0.8
GDP[d]	1.2×10^5 (± 0.05)	4.9×10^5 (± 0.4)	5.9×10^6 (± 0.2)	5.9×10^{10}	1.0
	1.3×10^5 (± 0.1)	2.4×10^7 (± 0.1)		3.2×10^{12}	1.1
GMPCP	1.1×10^5 (± 0.02)	3.0×10^5 (± 0.1)	3.2×10^6 (± 0.05)	3.2×10^{10}	0.7
	1.2×10^5 (± 0.2)	8.6×10^6 (± 0.7)		1.1×10^{12}	0.8
GMPCP*[c]	9.5×10^4 (± 0.4)	2.1×10^5 (± 0.2)	2.0×10^6 (± 0.07)	2.0×10^{10}	1.2
	1.1×10^5 (± 0.4)	4.1×10^6 (± 0.7)		4.6×10^{11}	1.3
ADP	1.2×10^5 (± 0.01)	3.5×10^5 (± 0.09)	4.2×10^6 (± 0.04)	4.2×10^{10}	1.4
	1.3×10^5 (± 0.3)	1.2×10^7 (± 0.2)		1.6×10^{12}	1.5
none	2.5×10^5 (± 0.03)	2.9×10^5 (± 0.09)	7.1×10^6 (± 0.08)	7.1×10^{10}	1.7
	2.9×10^5 (± 0.2)	8.0×10^6 (± 0.2)		2.3×10^{12}	1.8
		100 mM Pipes Buffer, 5.0 °C			
GTP	7.8×10^4 (± 0.2)	3.2×10^5 (± 0.1)	2.5×10^6 (± 0.04)	2.5×10^{10}	0.6
	8.9×10^4 (± 1.2)	9.8×10^6 (± 0.8)		8.7×10^{11}	0.7
GMPCPP	6.5×10^4 (± 0.6)	3.0×10^5 (± 0.5)	2.0×10^6 (± 0.3)	2.0×10^{10}	0.8
	7.6×10^4 (± 1.5)	8.9×10^6 (± 0.4)		6.8×10^{11}	0.9
GDP	6.0×10^4 (± 0.08)	6.5×10^5 (± 0.2)	3.8×10^6 (± 0.03)	3.8×10^{10}	1.6
	6.4×10^4 (± 1.3)	4.1×10^7 (± 0.6)		2.6×10^{12}	1.5
GMPCP	1.2×10^5 (± 0.04)	3.5×10^5 (± 0.2)	4.3×10^6 (± 0.1)	4.3×10^{10}	1.1
	1.4×10^5 (± 0.3)	1.2×10^7 (± 0.1)		1.7×10^{12}	1.2
GMPCP*[c]	2.0×10^5 (± 0.1)	2.7×10^5 (± 0.2)	5.5×10^6 (± 0.3)	5.5×10^{10}	0.7
	2.2×10^5 (± 0.3)	7.5×10^6 (± 0.4)		1.7×10^{12}	0.7
		100 mM Pipes, 19.7 °C			
GTP	8.4×10^4 (± 0.2)	5.2×10^5 (± 0.3)	4.3×10^6 (± 0.08)	4.3×10^{10}	1.1
	9.2×10^4 (± 0.2)	2.6×10^7 (± 0.03)		2.4×10^{12}	1.2
GMPCPP	1.1×10^5 (± 0.03)	4.2×10^5 (± 0.2)	4.5×10^6 (± 0.1)	4.5×10^{10}	1.2
	1.2×10^5 (± 0.2)	1.7×10^7 (± 0.2)		2.0×10^{12}	1.3
GDP	1.0×10^5 (± 0.02)	7.6×10^5 (± 0.2)	7.7×10^6 (± 0.1)	7.7×10^{10}	1.0
	1.1×10^5 (± 0.1)	5.7×10^7 (± 0.4)		6.1×10^{12}	1.1
GMPCP	1.1×10^5 (± 0.02)	7.0×10^5 (± 0.4)	7.6×10^6 (± 0.2)	7.6×10^{10}	1.7
	1.2×10^5 (± 0.2)	4.8×10^7 (± 0.5)		5.6×10^{12}	1.8
GMPCP*[c]	1.5×10^5 (± 0.05)	4.9×10^5 (± 0.2)	7.5×10^6 (± 0.2)	7.5×10^{10}	1.7
	1.7×10^5 (± 0.4)	2.4×10^7 (± 0.3)		4.0×10^{12}	1.7

[a] For each GXP entry, the first row was fit with the combined ligand-mediated plus ligand facilitated model; $K_4 = 1 \times 10^4$ M^{-1}. The second row was fit with the ligand-mediated model. [b] Vinblastine data from Lobert et al. (1) are reproduced here for clarity of presentation. [c] Tubulin was preequilibrated twice into buffers with 1 mM GMPCP as described in Materials and Methods. In the text and this table it is also labeled as GMPCP*. [d] Combined global analysis of data from this work and data from Lobert et al. (1).

all conditions studied (Figures 1A,B and 2). The mean $\Delta\Delta G(K_1K_2)$, averaged over all buffer and temperature conditions and corresponding to the difference between GMPCPP- and GTP-tubulin in overall affinity, K_1K_2, equals -0.06 (± 0.12) kcal/mol. This is summarized by the histograms in Figure 3A−C. Thus, we can conclude, from the perspective of vinblastine-induced spiral assembly, that GMPCPP is a perfect mimic of GTP. The structural differences and the conformational changes previously observed for GMPCPP- vs GTP-induced microtubule assembly compared polymerization processes that are linked to GTP hydrolysis (12−14). They compared the structure of GDP-microtubules with the structure of GMPCPP-microtubules. In the absence of GMPCPP hydrolysis, the observed differences are not surprising. However, GTP

hydrolysis does not occur in the vinblastine-induced self-association of tubulin, and therefore, here we are directly comparing GTP-tubulin with GMPCPP-tubulin.

Unlike GMPCPP, GMPCP differs in its effect on vinblastine-induced spiral assembly compared to its parental molecule GDP. Our initial experiments were performed in the usual manner by equilibrating GDP-tubulin into a 10 mM Pipes buffer containing 50 μM GMPCP plus varying vinblastine concentrations. This produced $\bar{s}_{20,W}$ data that was intermediate between those for GDP- and GTP-tubulin (see Figure 1A,B). However, due to the relatively low affinity of GMPCP for tubulin (11), this intermediate level could be due to a reduced ability to compete with endogenous GDP in the solution. When tubulin is equilibrated twice with 1 mM GMPCP and then equilibrated in the 50 μM GMPCP
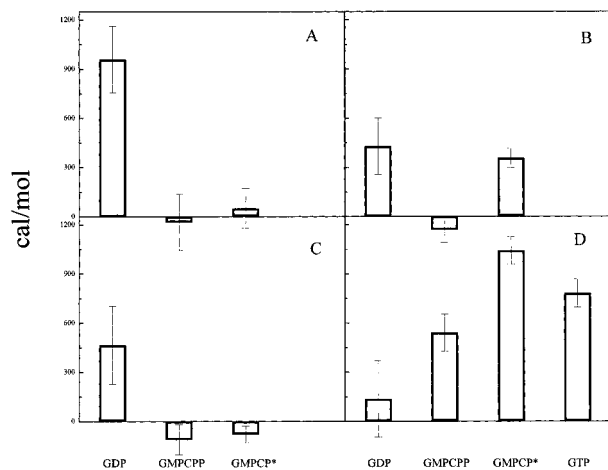
FIGURE 3: Histogram of $\Delta\Delta G(K)$ values, the difference between absolute values of free energy changes at different nucleotide and buffer concentrations. Individual values of the free energy change (ΔG) are calculated using data from Table 1 and the differences ($\Delta\Delta G$) are averaged for both models over two temperatures, unless indicated otherwise. Panel A: Nucleotide (GXP) enhancement in overall affinity relative to GTP, $\Delta\Delta G(K_1K_2) = \Delta\Delta G(K_1K_2)_{GXP} - \Delta\Delta G(K_1K_2)_{GTP}$ in 10 mM Pipes, 1 mM MgSO$_4$, 2 mM EGTA, and 50 μM GXP. Panel B: Nucleotide (GXP) enhancement in overall affinity relative to GTP, $\Delta\Delta G(K_1K_2) = \Delta\Delta G(K_1K_2)_{GXP} - \Delta\Delta G(K_1K_2)_{GTP}$ in 100 mM Pipes, 1 mM MgSO$_4$, 2 mM EGTA, and 50 μM GXP. Panel C: Nucleotide (GXP) enhancement in K_2 relative to GTP, $\Delta\Delta G(K_2) = \Delta\Delta G(K_2)_{GXP} - \Delta\Delta G(K_2)_{GTP}$ in 100 mM Pipes, 1 mM MgSO$_4$, 2 mM EGTA, and 50 μM GXP. Panel D: Enhancement caused by a change in Pipes concentration, $\Delta\Delta G(K_1K_2) = \Delta\Delta G(K_1K_2)_{GXP, 100\ mM\ Pipes} - \Delta\Delta G(K_1K_2)_{GXP, 10\ mM\ Pipes}$ at 5 °C. GMPCP* stands for additional equilibration of tubulin in 1 mM GMPCP-containing buffers, as described in Materials and Methods.

plus vinblastine-containing buffer (GMPCP*; see Materials and Methods), the $\bar{s}_{20,W}$ values now superimpose upon the data with GTP- and GMPCPP-tubulin. Thus, when partially exchanged, GMPCP-tubulin behaves in an intermediate manner between GDP- and GTP-tubulin (Figure 1A,B). When fully exchanged, GMPCP*-tubulin behaves exactly like GTP-tubulin. This is apparent in the overall affinity (Table 1). It is also very evident in a Wyman plot of the effective self-association constant ln K_2^{app} vs ln [vlb] (Figure 4A) and in the slope or linkage plot ΔX vs ln [vlb] (Figure 4B), where the values for GMPCP are intermediate between the data for GDP and the data for GTP and GMPCPP, while the data for GMPCP* superimpose on the GTP and GMPCPP data. When averaged over all models and temperatures, the mean difference in $\Delta\Delta G(K_1K_2)$ for GMPCP* relative to GTP is 0.05 ($\pm$0.10) kcal/mol (Figure 3A). In 10 mM Pipes we can conclude, from the perspective of vinblastine-induced spiral assembly, that GMPCP* is actually a mimic of GTP and GMPCPP. Thus, in low ionic strength buffer the α,β-methylene modification favors the GTP-tubulin conformation and induces GTP-like allosteric effects in the vinca-induced assembly of tubulin.

Our interpretation of the partially equilibrated GMPCP-tubulin data assumes this is an effect due to a mixture of GDP- and GMPCP-tubulin. An alternate possibility is that no GMPCP successfully competes with GDP, and the intermediate $\bar{s}_{20,W}$ level is due to the absence of excess GDP. To explore this possibility, control studies were performed with GDP-tubulin in the absence of excess nucleotide and in the presence of ADP, a nucleotide that binds weakly to a separate site on the tubulin heterodimer (21–23) or to the
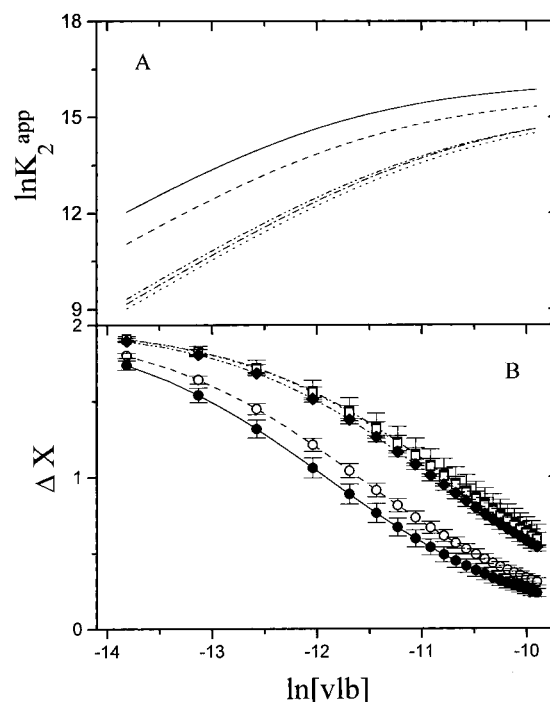

FIGURE 4: Wyman analysis of vinblastine binding to PC-tubulin in the presence of different nucleotides in 10 mM Pipes, 5 °C. K_2^{app} was calculated for 1.0–50 μM free vinblastine concentrations. Panel A shows plots of ln K_2^{app} vs ln [vlb] for spiral assembly in the presence of GDP (—), GMPCP (- - -), GTP (···), GMPCPP (— · —), and GMPCP* (— ·· —). Panel B plots the slopes of the lines in panel A (d ln K_2^{app}/d ln [X] = ΔX). The same lines used in panel A and the same symbols used in Figure 1 are used here for each nucleotide condition: GDP (●, —), GMPCP (○, — — —), GTP (■, ···), GMPCPP (□, — · —), GMPCP* (◆, — ·· —). In both panels partially exchanged GMPCP is clearly intermediate between GDP- and GTP-tubulin, while fully exchanged GMPCP*-tublin is identical to GTP- and GMPCPP-tubulin. The uncertainty in ΔX (error bars), derived from the propagated errors in K_1, is indicated in order to demonstrate that the difference observed are significant.

E-site when this site is depleted of guanine nucleotides (24, 25). These data are presented in Figure 1C. The results are intermediate between those obtained with GDP- and with partially equilibrated GMPCP-tubulin. This can be seen by a significant shift in the $\bar{s}_{20,W}$ plateau values obtained (Figure 1C) and in the overall binding affinities (Table 1). In overall binding affinities, we found that no nucleotide and ADP differ from partially equilibrated GMPCP by 0.46 $\pm$ 0.02 and 0.19 $\pm$ 0.03 kcal/mol, respectively. This means we cannot exclude a contribution from reduced E-site saturation with guanine nucleotides (26, 27). We can exclude a large nonspecific ionic strength contribution of 50 μM nucleotide to the self-association process since $\pm$ADP gives nearly identical results (see Figure 1C). ADP is known to induce tubulin ring formation, but this occurs at millimolar ADP concentrations, and there is no evidence for this effect occuring in the presence of vinblastine (21, 22). If there is an ADP effect under these conditions it is obviously small.

The previous structural and assembly studies of GMPCPP-induced microtubule assembly were primarily performed in 100 mM Pipes buffers. To relate our study of GMPCP and GMPCPP to similar conditions, we repeated our experiments in 100 mM Pipes buffer. [It has been reported that zwitterions at this concentration induce weak tubulin self-association with a K_d for dimerization of 2.6 mM (28). All of the experimental $\bar{s}_{20,W}$ data presented here extrapolates to
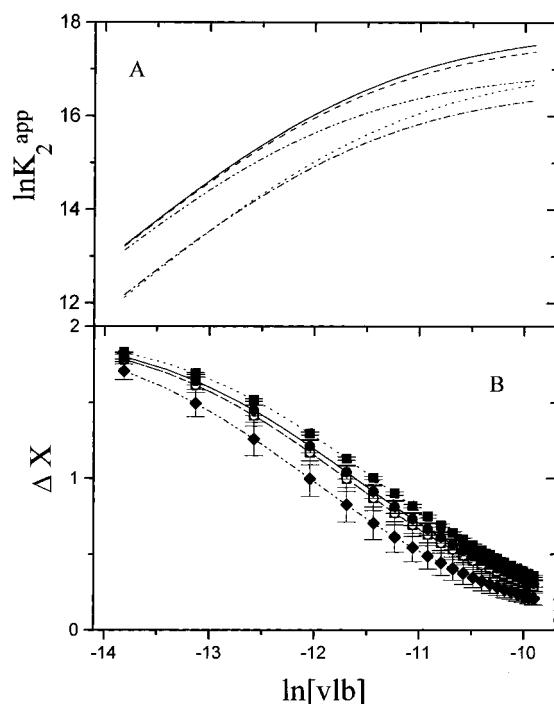
FIGURE 5: Wyman analysis of vinblastine binding to PC-tubulin in the presence of different nucleotides in 100 mM Pipes, 19.7 °C. K_2^{app} was calculated for 1.0−50 μM free vinblastine concentrations. Panel A shows plots of ln K_2^{app} vs ln [vlb] for spiral assembly in the presence of GDP (−), GMPCP (− − −), GTP (···), GMPCPP (− · −), and GMPCP* (− ·· −). The GMPCP* data are relatively intermediate between GDP- and GTP-tubulin. Panel B plots the slopes of the lines in panel A (d ln K_2^{app}/d ln[X] = ΔX). The same lines used in panel A and the same symbols used in Figure 2 are used here for each nucleotide condition: GDP (●, −), GMPCP (○, − − −), GTP (■, ···), GMPCPP (□, − · −), and GMPCP* (◆, − ·· −). The uncertainty in ΔX (error bars), derived from the propagated errors in K_1, is indicated in order to demonstrate that the difference observed with GMPCP* is significant.

5.8S, the sedimentation coefficient of the tubulin heterodimer (Figures 1 and 2). Thus, under our conditions (2 μM tubulin; see Materials and Methods and below) there is no evidence of tubulin self-association in the absence of drug.] GMPCPP strongly nucleates microtubule assembly and, above 20 °C, induces microtubule formation at 2 μM tubulin, our typical solution conditions. Thus, these studies were performed at 5 and 19.7 °C. As described above, GMPCPP is a perfect mimic of GTP under all solution conditions studied. In 100 mM Pipes, GMPCP mimics GDP in overall binding affinities [mean $\Delta\Delta G(K_1K_2)$ equals −0.02 (±0.17) kcal/mol], although there are significant differences in the extent of self-association, as seen by a lack of superposition in the $\bar{s}_{20,w}$ data (Figure 2A,B) and significantly lower K_2 values (Table 1, Figure 3C). Both the partially exchanged (GMPCP) and the fully exchanged (GMPCP*) samples exhibit significantly reduced $\bar{s}_{20,w}$ plateau values. This is especially evident in the 5 °C data (Figure 2A). This suggests that raising the ionic strength of the buffer partially converts GMPCP-tubulin to the GDP-tubulin conformation, consistent with the previous observation that GTP-tubulin differs from GDP-tubulin by electrostatic strain that is overcome by raising the salt concentration (8). This is verified by the overall enhancement of spiral assembly in 100 mM Pipes buffer induced by GMPCP relative to GTP [$\Delta\Delta G(K_1K_2) = 0.36$ (±0.06) kcal/mol]. This is more evident in a Wyman plot of the effective self-association constant, ln K_2^{app} vs ln [vlb] (Figure 5A),

where the ln K_2^{app} values for GMPCP* are relatively intermediate between the data for GDP and the data for GTP and GMPCPP.

DISCUSSION

By the criterion of vinblastine-induced spiral assembly, GMPCPP is a perfect GTP analogue. There is no significant difference in overall binding (average $\Delta\Delta G(K_1K_2)$ for both models equals −0.06 ± 0.13 kcal/mol), or in individual binding parameters [average $\Delta\Delta G(K_1)$, $\Delta\Delta G(K_2)$, and $\Delta\Delta G(K_3)$ for both models are 0.04 ± 0.10, −0.10 ± 0.14, and −0.06 ± 0.13 kcal/mol, respectively]. This is somewhat different from what we have seen by van't Hoff analysis of microtubule polymerization (12) and what others have seen by structural analysis (13, 14). It is possible that lateral interactions in the microtubule lattice account for this difference. However, in all those studies GMPCPP-microtubules were being compared to a GDP-microtubule lattice, while in our studies, since no hydrolysis occurs during vinblastine-induced assembly, we are comparing GMPCPP- with GTP-tubulin. This would argue that GMPCPP is a GTP analogue and the previous observations correctly identified differences between a GMPCPP- and a GDP-microtubule lattice. The similarity we observe between GMPCP- and GTP- or GMPCPP-tubulin suggests that even if a small amount of hydrolysis occurs during microtubule assembly, forming GMPCP-tubulin, the lattice will maintain a partial GTP-like topology. This is verified by the significant differences observed by van't Hoff analysis of GMPCP-induced microtubule polymerization compared to GTP-induced polymerization (12). It is not presently known how tightly coupled the structure of the macromolecular lattice is to nucleotide-induced conformational changes. High-resolution structural information, currently not available (29, 30), is required to distinguish between changes in lattice topology from changes in the tubulin heterodimer conformation. Temperature-dependent changes in the pitch of vinblastine-induced GTP-tubulin spiral structure has been measured by time-resolved X-ray solution scattering (31). Similar studies as a function of the tubulin-nucleotide state are readily feasible and might be very informative.

As reported earlier (1, 2, 8), GDP enhances vinca alkaloid-induced tubulin self-association. The larger overall binding affinity arises from larger values of K_2, the binding of liganded heterodimers to spirals, and K_3, the binding of a drug to polymers. [While there are changes in K_1, the average values, (0.93 ± 0.51) × 10⁵ M⁻¹ at 5 °C and (1.23 ± 0.47) × 10⁵ M⁻¹ at 20−25 °C, are within our previous range of determinations for vinblastine (1, 2) and not considered significantly different.] The mean enhancement for GDP vs GTP spiral assembly in 10 mM Pipes is 0.96 ± 0.20 kcal/mol compared to 0.43 ± 0.17 kcal/mol in 100 mM Pipes. This reduction in GDP enhancement with an increase in Pipes concentration is similar to the effect seen when NaCl is added to the assembly buffer (8). In fact, 150 mM NaCl caused a reduction in GDP enhancement of 0.51 kcal/mol, which is similar to the 0.53 kcal/mol reduction in enhancement seen upon addition of 100 mM of Pipes. Since GMPCPP perfectly mimics GTP by the criterion of vinblastine-induced assembly, then it is not surprising that GDP enhances spiral assembly relative to GMPCPP to the same extent (0.99 ± 0.23 kcal/mol in 10 mM Pipes and 0.51 ± 0.21 kcal/mol in 100 mM Pipes). We assume that increasing

concentrations of both NaCl and Pipes are nonspecifically overcoming an electrostatic inhibition in the GTP- or GMPCPP-tubulin state that is unfavorable for spiral formation. Note that the Pipes buffer is titrated with NaOH to the desired pH value and there is an appreciable increase in [Na$^+$] in the solutions as well. We cannot distinguish between a salt effect, a cation effect, an anion effect, or a nonspecific ionic strength effect, but for simplicity we refer to this as a salt effect.

The enhancement of spiral assembly by an increase in Pipes concentration is represented by a histogram of $\Delta\Delta G$ values in Figure 3D. Here we compare the overall affinity in the presence of 100 mM Pipes relative to 10 mM Pipes under identical nucleotide conditions. The smallest ionic strength enhancement occurs with GDP-tubulin (0.14 ± 0.23 kcal/mol), while the largest enhancement occurs with GMPCP*-tubulin (1.04 ± 0.08 kcal/mol). We have interpreted the enhancement observed with GTP- and GMPCPP-tubulin to be due to overcoming an unfavorable electrostatic interaction in the GTP state. The enhancement of GDP-tubulin spiral assembly by increasing the Pipes or NaCl concentration probably reflects a small nonspecific preferential interaction of the buffer or salt with spirals (8, 32). The additional enhancement observed with GMPCP*-tubulin may represent a salt-induced conformational change that partially mimics the GDP state. This would reflect overcoming both electrostatic strain and additional conformational restraints. The absence of a γ-phosphate may allow for this salt-induced conversion from GTP- to a partial GDP-tubulin conformation. We cannot exclude an ordered linkage between spiral assembly and this more favorable conformation. The conversion is not complete as evidenced by a plateau in $\bar{s}_{20,w}$ values that are intermediate between GDP- and GTP-tubulin. This is also seen in the ln K_2^{app} vs ln [vlb] plots (Figure 5) where the effective K_2^{app} for GMPCP* is near GDP-tubulin at low drug concentration and near GTP- and GMPCPP-tubulin at higher drug concentration. Inspection of the $\bar{s}_{20,w}$ vs vinblastine concentration plots (Figure 2) reveal the same trend. This suggests that the α,β-methylene contributes some additional unfavorable energy to spiral formation even in high salt.

Nonhydrolyzable nucleotide analogues have been used extensively to investigate the role of GTP hydrolysis in microtubule assembly (9−14, 23, 24). More recently GMPCPP was used to study the interaction of kinesin motor domain constructs with stabilized microtubules (13). The interpretation of all these data requires that the analogues are true mimics of the parent molecules and do not induce alternate conformations in the microtubule lattice. Our recent study suggested, by van't Hoff analysis of microtubule assembly, that GMPCP and GMPCPP may not be true GDP and GTP analogues (12). We have extended this study to a direct quantitative test using sedimentation velocity analysis of nucleotide-enhanced vinblastine-induced spiral formation. We conclude that an α,β-methylene in guanine nucleotides favors the GTP-tubulin state in a salt concentration-dependent manner. This has implications for the molecular interpretation of structural data collected with these analogues. It also demonstrates the exquisite sensitivity with which the E-site of tubulin senses modifications in the guanine nucleotide ligand and translates them into allosteric effects. This indicates the potential to probe allosteric effects and effectors in the tubulin system by quantitative studies of vinca
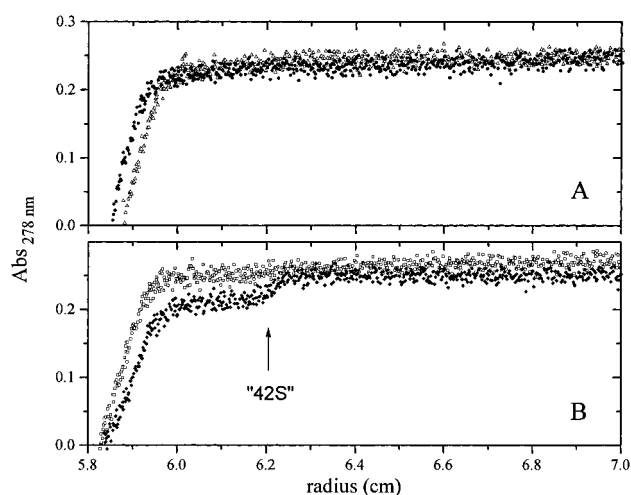

FIGURE 6: Radial scans at 278 nm of tubulin solutions sedimenting at 30K rpm in the XLA analytical ultracentrifuge. Buffer and temperature conditions are 10 mM Pipes, 2 mM EGTA, pH 6.9, 16 mM MgSO$_4$, and 50 μM GXP, 5 °C. Panel A: GMPCPP ($\bullet$) (1868 s into the run) and GMPCP* ($\blacktriangle$) (1975 s). Panel B: GTP ($\square$) (2992 s) and GDP ($\blacklozenge$) (2888 s). Analysis by DCDT reveals that a 42S boundary is present only in the GDP-tubulin sample (indicated in panel B). This demonstrates that GDP-tubulin strongly facilitates the fomation of Mg^{+2}-induced rings, while GTP-, GMPCPP-, and GMPCP-tubulin do not. [Note that these experiments were done at 5 °C because the increase in [Mg^{+2}] favors GMPCPP-induced microtubule formation, thus complicating the interpretation.]

alkaloid-induced spiral assembly. This work and our previous studies (1, 2, 8) place the vinca alkaloid-tubulin system complementary to Mg^{+2}-induced ring formation (33, 34) and microtubule assembly (12, 32) for investigating the role of nucleotides on tubulin. GDP-tubulin favors ring formation, while GTP-tubulin favors microtubule assembly. We are currently conducting an extensive investigation of the influence of other divalent cations on tubulin ring formation. As an extension to these nucleotide analogue studies we performed preliminary experiments on the ability of GMPCPP- and GMPCP-tubulin to form Mg^{+2}-induced rings. As shown in Figure 6, and consistent with our observations on GMPCP-tubulin and vinblastine, only GDP-tubulin readily forms a 42S boundary, indicating the formation of a Mg^{+2}-induced double-walled ring. Thus, our observations with GMPCP and vinblastine-induced self-association are confirmed by Mg^{+2}-induced ring formation. This verifies our assertion that multiple modes of tubulin self-association can be utilized to probe allosteric effects of nucleotides and antimitotic drugs (32).

ACKNOWLEDGMENT

REFERENCES

1. Lobert, S., Frankfurter, A., and Correia, J. J. (1995) *Biochemistry 34*, 8050−8060.
2. Lobert, S., Vulevic, B., and Correia, J. J (1996) *Biochemistry 35*, 6806−6814.
3. Himes, R. H. (1991) *Pharmacol. Ther. 51*, 257−267.

4. Dhamodharan, R., Jordan, M. A., Thrower, D., Wilson, L., and Wadsworth, P. (1995) *Mol. Biol. Cell 6*, 1215−1229.

5. Singer, W. D., Hersh, R. T., and Himes, R. H.. (1988) *Biochem. Pharmacol. 37*, 2691−2696.

6. Na, G. C., and Timasheff, S. N. (1986) *Biochemistry 25*, 6214−6222.

7. Na, G. C., and Timasheff, S. N. (1986) *Biochemistry 25*, 6222−6228.

8. Lobert, S., Boyd, C. A., and Correia, J. J. (1997) *Biophys. J. 72*, 416−427.

9. Hyman, A. A., Salser, S., Drechsel, D. N., Unwin, N., and Mitchison, T. J. (1992) *Mol. Biol. Cell 3*, 1155−1167.

10. Caplow, M. (1992) *Curr. Opin. Cell Biol. 4*, 58−65.

11. Caplow, M., Ruhlen, R. L., and Shanks, J. (1994) *J. Cell Biol. 127*, 779−788.

12. Vulevic, B., and Correia, J. J. (1997) *Biophys. J. 72*, 1357−1375.

13. Vale, R. D., Coppin, C. M., Malik, F., Kull, F. J., and Milligan, R. A. (1994) *J. Biol. Chem. 269*, 23769−23775.

14. Hyman, A. A., Chretien, D., Arnal, I., and Wade, R. H. (1995) *J. Cell Biol. 128*, 117−125.

15. Williams, R. C. Jr., and Lee, J. C.(1982) *Methods Enzymol. 85*, 376−408.

16. Correia, J. J., Baty, L. T., and Williams, R. C., Jr. (1987) *J. Biol. Chem. 262*, 17278−17284.

17. Detrich, H. W., and Williams, R. C., Jr. (1978) *Biochemistry 17*, 3900−3907.

18. Correia, J. J., Beth, A. H., and Williams, R. C., Jr. (1988) *J. Biol. Chem. 263*, 10681−10686.

19. Liu, S., and Stafford, W. F., III (1995) *Anal. Biochem. 224*, 199−202.

20. Stafford, W. F., III (1992) *Anal. Biochem. 203*, 295−301.

21. Zabrecky, J. R., and Cole, R. D. (1982) *Nature 296*, 775−776.

22. Zabrecky, J. R., and Cole, R. D. (1982) *J. Biol. Chem. 257*, 4633−4638.

23. O'Brien, E. T., and Erickson, H. P. (1989) *Biochemistry 28*, 1413−1422.

24. Seckler, R., Wu, G.-M., and Timasheff, S. N. (1990) *J. Biol. Chem. 265*, 7655−7661.

25. Hanssens, I., Baert, J., and Van Cauwelaert, F. (1990) *Biochemistry 29*, 5160−5165.

26. Croom, H. B., Correia J. J., Baty L. T., and Williams, R. C., Jr. (1985) *Biochemistry 24*, 768−775.

27. Croom, H. B., Correia, J. J., and Williams, R. C., Jr. (1986) *Arch. Biochem. Biophys. 249* , 397−406.

28. Foster, K. E., and Rosenmeyer, M. A. (1986) *FEBS Lett. 194*, 78−84.

29. Nogales, E., Wolf, S. G., Khan, I. A., Luduena, R. F., and Downing, K. H. (1995) *Nature 375*, 424−427.

30. Wolf, S. G., Nogales, E., Kikkawa, M., Gratzinger, D., Hirokawa, N., and Downing, K. H. (1996) *J. Mol. Biol. 262*, 485−501.

31. Nogales, E., Medrano, F. J., Diakun, G. P., Mant, G. R., Towns-Andrews, E., and Bordas, J. (1995) *J. Mol. Biol. 254*, 416−430.

32. Correia, J. J. (1991) *Pharmacol. Ther. 52*, 127−147.

33. Frigon, R. P., and Timasheff, S. N. (1975) *Biochemistry 14*, 4559−4566.

34. Frigon, R. P., and Timasheff, S. N. (1975) *Biochemistry 14*, 4567−4573.